

# Experimental Study on Line-of-Sight (LOS) Attitude Control Using Control Moment Gyros under Micro-Gravity Environment

By Hirohisa KOJIMA<sup>1)</sup>, Kana HIRAIWA,<sup>1)</sup> Yasuhiro YOSHIMURA,<sup>1)</sup> and Koki HIDAKA<sup>1)</sup>

<sup>1)</sup>Department of Aerospace Engineering, Tokyo Metropolitan University, Hino, Japan

This paper presents the results of line-of-sight (LOS) attitude control using control moment gyros under a micro-gravity environment generated by parabolic flight. The  $W$ - $Z$  parameters are used to describe the spacecraft attitude. In order to stabilize the current LOS to the target LOS, backstepping-based feedback control is considered using the  $W$ - $Z$  parameters. Numerical simulations and experiments under a micro-gravity environment are carried out, and their results are compared in order to validate the proposed control methods.

**Key Words:**  $W$ - $Z$  parameters, Control Moment Gyro, Line of Sight, Attitude Maneuver

## Nomenclature

$A$	: Jacobian matrix for 2SGCMGs
$\tilde{A}$	: Jacobian matrix for LOS control
$C$	: Jacobian matrix for 4SGCMGs
$[a \ b \ c]^T$	: directional cosine vector of the $Z$ -axis with body axes
$H$	: CMG angular momentum vector
$H_i$	: $i$ -th CMG angular momentum vector
$h_0$	: angular momentum of the CMG wheel
$J$	: satellite inertia tensor (= $\text{diag}(J_x, J_y, J_z)$ )
$J_w$	: moment of inertia of the CMG wheel about the spin axis
$\tilde{J}$	: part of satellite inertia tensor(= $\text{diag}(J_x, J_y)$ )
$k_1, k_2, k_3$	: control gains
$(X, Y, Z)$	: inertial coordinate axes
$(X_b, Y_b, Z_b)$	: satellite body axes
$(X_c, Y_c, Z_c)$	: CMG axes
$w_1, w_2, z$	: $W$ - $Z$ parameters
$w$	: $W$ parameter vector (= $[w_1 \ w_2]^T$ )
$\beta$	: skew angle (= 54.73 deg)
$\delta$	: gimbal angle vector (= $[\delta_1 \ \delta_2 \ \delta_3, \delta_4]^T$ )
$\delta_i$	: gimbal angle ( $i = 1, 2, 3, 4$ )
$\Omega$	: rotational speed of the CMG wheel
$\omega$	: angular velocity of the spacecraft in the body frame (= $[\omega_1 \ \omega_2 \ \omega_3]^T$ )
$\tilde{\omega}$	: two-dimensional angular velocity of the spacecraft in the body frame(= $[\omega_1 \ \omega_2]^T$ )
$\tau$	: attitude control torque generated by CMGs
$\bar{*}$	: complex conjugate of a complex number *

## 1. Introduction

Control moment gyros (CMGs) are attitude control actuators. An advantage of CMG systems is that they can generate higher torque than reaction wheels (RWs) and are therefore used in large spacecraft such as the International Space Station (ISS). Unlike RWs, however, CMGs contain motorized actuators known as gimbals. The presence of gimbals introduces the risk of failure, and additional redundancy is required

in the attitude controller in order to ensure controllability, since post-launch repair is generally impossible. Although this redundancy increases fault tolerance, it also increases the spacecraft weight. Even if one or more CMGs malfunction, satellites must maintain attitude control as much as possible. Many studies have examined methods by which to provide acceptable levels of fault tolerance without additional weight as a solution to the problem of maintaining three-axis attitude control in the event of the failure of one or more actuator. In one form of the under-actuated control problem, known as the two-torque problem,<sup>1)</sup> the goal is to damp out the rotational motion<sup>2-10)</sup> and/or maintain three-axis attitude control<sup>11-19)</sup> when torque can be generated only around two axes.

Most studies have assumed the use of thrusters or two orthogonal RWs, or have taken similar approaches, but a few studies, considered the use of two single-gimbal control moment gyros (SGCMGs). For example, Kwon et al.<sup>20)</sup> studied linear parameter-varying (LPV) control, Gui et al.<sup>21)</sup> studied singular-value decomposition, and Gui et al.<sup>22)</sup> investigated the modified direct-inverse steering law, where two parallel SGCMG gimbal axes were assumed in all of these studies. As long as their angular momenta are not parallel, two parallel gimbal axes can generate two-axis torque in a manner similar to that for attitude control using two orthogonal RWs. In the widely used pyramid-array SGCMG system, however, the failure of two CMGs will not leave two functioning CMGs with parallel gimbal axes. In a skewed array, moreover, the independent degrees of freedom of the two SGCMGs are those of the two gimbals, but the generated torque is three dimensional. With skewed-axis CMGs, it is therefore not possible to obtain control simply by applying two-axis torque in the manner of two orthogonal RWs or two CMGs with parallel gimbal axes. Yamada et al.<sup>23)</sup> studied rate damping control using two SGCMGs. Kasai et al.<sup>24)</sup> proposed a three-axis attitude control method for two skewed CMGs, using the coming effect of repeated one-axis maneuvering with a built-in gimbal-rate limiter. However, its range of applications is limited because control is achieved by feedforward control. Gui et al.<sup>25)</sup> proposed feedback control using a generalized dynamic inverse (GDI) procedure for orientations that depart substantially from the target attitude, together with

backstepping control for stabilization to the target attitude. In all cases, however, three-axis attitude control with two skewed SGCMGs using feedback control has invariably required complex nonlinear control techniques.

Line-of-sight (LOS) control is widely used in astronomical observations and communications to point the mission equipment in a specified direction for astronomical body observation or communication. In many cases, the conditions for attitude stabilization around the LOS axis in a specified direction can be relaxed, and LOS control by two skewed SGCMGs may therefore be easier than three-axis attitude control. In Ref. 26), LOS attitude maneuver control consisting of two phases is proposed using the  $W$ - $Z$  parameters for describing the spacecraft attitude. The expression in terms of the  $W$ - $Z$  parameters is suitable for two-axis (LOS) attitude maneuver control. However, most previous studies on two-skewed CMGs involved numerical simulations, and experimental studies have not yet been adequately performed. This is because the three-dimensional attitude motion of a satellite model is not easy to control in an arbitrary direction on the ground due to the effect of gravity. Several techniques have been developed to realize three-dimensional motion on the ground, including air-bearing simulators<sup>28)</sup> and micro-gravity conditions using parabolic flight<sup>29)</sup> or free fall. Air-bearing simulators are widely used and can realize long-duration experiments, but cannot achieve complete three-dimensional motion due to the presence of a pillar. In contrast, parabolic flight or free fall can provide completely three-dimensional free space, but cannot be used in long-duration experiments.

In this study, prioritizing the three-dimensional motion over the duration of experiments, attitude maneuvering experiments are carried out under micro-gravity environments in order to validate the backstepping-based steering control of two skewed SGCMGs for LOS attitude maneuvering using  $W$ - $Z$  parameters.<sup>27)</sup> The results of numerical simulations and experiments are then compared in order to confirm the validity of the steering control and LOS attitude maneuvering experimentally.

The remainder of this paper is organized as follows. In Section 2, the pyramid-type CMG system is explained. The attitude as expressed using  $W$ - $Z$  parameters is described in Section 3. The steering control law for two-skewed CMGs and steering law for damping rotation about the LOS axis are derived in Section 4. In order to validate the steering control laws, numerical and experimental results are presented and compared in Section 5. Section 6 presents the conclusions of this study.

## 2. Pyramid-type CMGs

### 2.1. Four CMGs

Figure 1 shows a schematic diagram of the pyramid arrangement of four SGCMGs considered in this study. The  $X_c$ ,  $Y_c$ , and  $Z_c$  axes correspond to the CMG axes. The vector  $\mathbf{g}_i$  represents the direction of the  $i$ -th CMG gimbal axis.

The gimbal angle for each CMG is denoted as  $\delta_i$ . In a traditional pyramid-type CMG system, the skew angle  $\beta$  is fixed at  $\beta = \tan^{-1} \sqrt{2}$  rad ( $= 54.73$  deg), because the momentum envelope representing the maximum available angular momentum of the CMG for attitude maneuvers becomes nearly spherical for

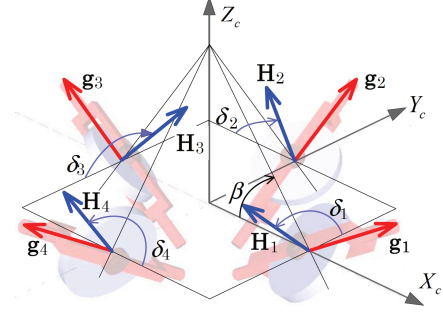


Fig. 1. Pyramid arrangement of four SGCMGs.

the case of this skew angle. The total CMG angular momentum vector for the four SGCMGs  $\mathbf{H}$  is expressed in the CMG coordinate system as

$$\mathbf{H} = \sum_{i=1}^4 \mathbf{H}_i(\delta_i) = h_0 \begin{bmatrix} -c\beta \sin \delta_1 \\ \cos \delta_1 \\ s\beta \sin \delta_1 \end{bmatrix} + h_0 \begin{bmatrix} -\cos \delta_2 \\ -c\beta \sin \delta_2 \\ s\beta \sin \delta_2 \end{bmatrix} + h_0 \begin{bmatrix} c\beta \sin \delta_3 \\ -\cos \delta_3 \\ s\beta \sin \delta_3 \end{bmatrix} + h_0 \begin{bmatrix} \cos \delta_4 \\ c\beta \sin \delta_4 \\ s\beta \sin \delta_4 \end{bmatrix} \quad (1)$$

where  $c\beta = \cos \beta$ , and  $s\beta = \sin \beta$ .

The time derivative of the angular momentum vector for the CMGs can be obtained as

$$\dot{\mathbf{H}} = \sum_{i=1}^4 \frac{\partial \mathbf{H}_i}{\partial \delta_i} \dot{\delta}_i = \mathbf{f}_1 \dot{\delta}_1 + \mathbf{f}_2 \dot{\delta}_2 + \mathbf{f}_3 \dot{\delta}_3 + \mathbf{f}_4 \dot{\delta}_4 = h_0 \mathbf{C} \dot{\boldsymbol{\delta}} \quad (2)$$

where

$$\mathbf{C} = \begin{bmatrix} \mathbf{f}_1 & \mathbf{f}_2 & \mathbf{f}_3 & \mathbf{f}_4 \end{bmatrix} = \begin{bmatrix} -c\beta \cos \delta_1 & \sin \delta_2 & c\beta \cos \delta_3 & -\sin \delta_4 \\ -\sin \delta_1 & -c\beta \cos \delta_2 & \sin \delta_3 & c\beta \cos \delta_4 \\ s\beta \cos \delta_1 & s\beta \cos \delta_2 & s\beta \cos \delta_3 & s\beta \cos \delta_4 \end{bmatrix}. \quad (3)$$

When the CMG system is in the singular state, the CMG cannot produce torque about the direction of vector  $\mathbf{s}$  perpendicular to the plane of  $\dot{\mathbf{H}}$ , regardless of the gimbal rate. This situation occurs when  $\dot{\mathbf{H}}$  from Eq. (2) lies in a plane for any choice of  $\dot{\boldsymbol{\delta}}$ . The corresponding gimbal angles, momentum vector, and vector  $\mathbf{s}$  are called the singular gimbal angles, singular momentum vector, and singular vector, respectively.

### 2.2. Two CMGs

When we assume that two mutually opposed CMGs (Nos. 2 and 4) in the pyramid array of four CMGs have failed and possess no angular momentum, the CMG system can be considered to be a two-skewed SGCMG system, as shown in Fig. 2. In this case, the angular momentum in the CMG system is given by

$$\mathbf{H} = \sum_{i=1,3} \mathbf{H}_i(\delta_i) = h_0 \begin{bmatrix} -c\beta \sin \delta_1 \\ \cos \delta_1 \\ s\beta \sin \delta_1 \end{bmatrix} + h_0 \begin{bmatrix} c\beta \sin \delta_3 \\ -\cos \delta_3 \\ s\beta \sin \delta_3 \end{bmatrix} \quad (4)$$

We now consider the time derivative of the angular momentum of two SGCMGs.

$$\dot{\mathbf{H}} = \sum_{i=1,3} \dot{\mathbf{H}}_i = h_0 \mathbf{A} \begin{bmatrix} \dot{\delta}_1 \\ \dot{\delta}_3 \end{bmatrix} \quad (5)$$

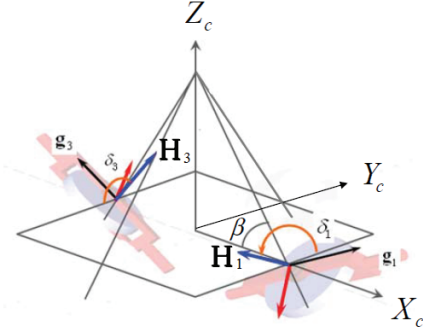


Fig. 2. Two skewed SGCMGs.

where  $A$  is the Jacobian matrix given by

$$A = \begin{bmatrix} -c\beta \cos \delta_1 & c\beta \cos \delta_3 \\ -\sin \delta_1 & \sin \delta_3 \\ s\beta \cos \delta_1 & s\beta \cos \delta_3 \end{bmatrix}. \quad (6)$$

Since the attitude control torque, which is generated by the CMGs and applied to the spacecraft, is opposite the time-derivative of the CMG angular momentum for the case of single spin, the attitude control torque generalized by the CMGs for the case of single spin can be written as

$$\tau = -\dot{\mathbf{H}} = -\sum_{i=1,3} \dot{\mathbf{H}}_i = -h_0 A \begin{bmatrix} \dot{\delta}_1 \\ \dot{\delta}_3 \end{bmatrix} \quad (7)$$

When the gimbals are actuated at  $[\delta_1 \ \delta_3] = [\delta \ \delta]$  with  $[\dot{\delta}_1 \ \dot{\delta}_3] = [-\dot{\delta} \ -\dot{\delta}]$ , the generated torque is

$$\tau = -\dot{\mathbf{H}} = h_0 \begin{bmatrix} 0 & 0 & 2\dot{\delta}s\beta \cos \delta \end{bmatrix}^T \quad (8)$$

and torque can be generated only about the  $Z_c$ -axis. Conversely, if they are actuated at  $[\delta_1 \ \delta_3] = [\delta \ -\delta]$  with  $[\dot{\delta}_1 \ \dot{\delta}_3] = [\dot{\delta} \ -\dot{\delta}]$ , we have

$$\tau = -\dot{\mathbf{H}} = h_0 \begin{bmatrix} 2\dot{\delta}c\beta \cos \delta & 0 & 0 \end{bmatrix}^T \quad (9)$$

and torque can be generated only about the  $X_c$ -axis.

### 3. W-Z Parameters

The attitude of a spacecraft may be expressed in terms of Euler angles, quaternions, Rodrigues parameters, or various other parameters. In this study, we use the  $W$ - $Z$  parameters proposed by Tsiotras and Longuski.<sup>27)</sup> In this section, we describe how these parameters are used for attitude expression and why they are suitable for LOS control.

The  $W$ - $Z$  parameters express the attitude in terms of two rotational transforms (see Fig. 3). The first is a rotation  $z$  about the  $Z$ -axis. The second is a rotation  $\theta$  about a vector  $\mathbf{u}$  in the  $X$ - $Y$  plane to match the attitude. Let us denote the directional cosine vector of the axis  $Z$  with the body axes  $(X_b, Y_b, Z_b)$  as  $[a \ b \ c]^T$ , as shown in Fig. 3. Defining the vector  $\mathbf{w}$  as

$$\mathbf{w} = \begin{bmatrix} \frac{b}{1+c} & \frac{-a}{1+c} \end{bmatrix}^T = [w_1 \ w_2]^T \quad (10)$$

we then have the following relation between the time derivatives of the  $W$ - $Z$  parameters and the angular velocity of the satellite:

$$\begin{bmatrix} \dot{w}_1 \\ \dot{w}_2 \\ \dot{z} \end{bmatrix} = \begin{bmatrix} (1 + w_1^2 - w_2^2)/2 & w_1 w_2 & w_2 \\ w_1 w_2 & (1 - w_1^2 + w_2^2)/2 & -w_1 \\ -w_2 & w_1 & 1 \end{bmatrix} \begin{bmatrix} \omega_1 \\ \omega_2 \\ \omega_3 \end{bmatrix} \quad (11)$$

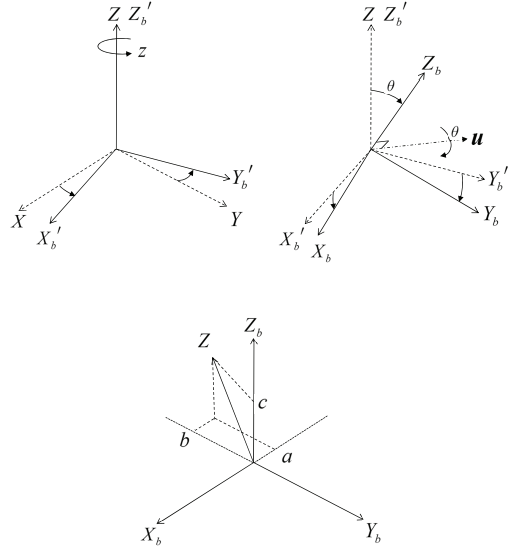


Fig. 3. Definition of  $W$ - $Z$  parameters.

Rewriting vector  $\mathbf{w}$  in complex-number notation as

$$\hat{w} = w_1 + iw_2 \quad (12)$$

and similarly rewriting the satellite's angular velocity components on the  $x$  and  $y$  axes as

$$\hat{\omega} = \omega_1 + i\omega_2, \quad (13)$$

we can then rewrite Eq. (11) as

$$\dot{\hat{w}} = -i\omega_3 \hat{w} + \frac{\hat{\omega}}{2} + \left(\frac{\tilde{\omega}}{2}\right) \hat{w}^2, \quad (14)$$

$$\dot{z} = \omega_3 + \text{Im}(\hat{\omega} \tilde{\hat{w}}). \quad (15)$$

In considering LOS control, if we take the direction of the mission equipment as the  $Z_b$ -axis in the satellite's body coordinate system, it is then not necessary to restrict the attitude about the  $Z_b$ -axis, and, consequently, it is not necessary to control the value of  $z$  in the  $W$ - $Z$  parameters. The control problem is thereby reduced to a problem of stabilizing the two-dimensional vector  $\mathbf{w}$  to zero. Based on Eq. (14), the time derivative of the squared norm of  $\mathbf{w}$  is then

$$\frac{d}{dt} |\hat{w}|^2 = (1 + |\hat{w}|^2) \text{Re}(\hat{\omega} \tilde{\hat{w}}), \quad (16)$$

$$\frac{d}{dt} |\mathbf{w}|^2 = (1 + |\mathbf{w}|^2) (\tilde{\omega} \cdot \mathbf{w}). \quad (17)$$

The  $W$ - $Z$  parameters are complex numbers, but, as shown in Eq. (16) or Eq. (17), the time derivative of  $|\mathbf{w}|$ , which represents the LOS angle, can be expressed by only a real value. The  $W$ - $Z$  parameters are therefore appropriate for LOS control, and, in this study, we take Eq. (16) or Eq. (17) as the basis for designing a feedback controller. The  $W$ - $Z$  parameters are conceived as expressions for application to the two-torque problem, in which torque cannot be generated about the  $Z_b$ -axis. In order to simplify the application of the  $W$ - $Z$  parameters to the LOS attitude maneuver problem using CMGs, we hereinafter assume that the  $X_c$ - and  $Z_c$ -axes of the CMG coordinate system coincide with

the  $X_b$ - and  $Y_b$ -axes, respectively, of the satellite's body coordinate system.

#### 4. Line-of-Sight Control

##### 4.1. Steering control law with two gimbals for LOS axis maneuvering

The use of just one nonlinear feedback controller to perform attitude control (three-axis or LOS) is desirable since it eliminates the need to switch between two controllers, but nonlinear feedback control tends to require control quantities exceeding the actuator limit, with the attendant difficulty of designing a gain that would prevent limit overruns.

In this study, we assume that the angular momentum of the overall system is zero. Near the target LOS attitude, we assume that if gyration has sufficiently slowed, then the two gimbal angles of the two skewed SGCMGs are both close to 0 or 180 deg. The angular momentum of the CMG system as expressed in the satellite's body coordinate system is then

$$\mathbf{H} \approx h_0 \begin{bmatrix} -c\beta(\sin \delta_1 - \sin \delta_3) \\ s\beta(\sin \delta_1 + \sin \delta_3) \\ 0 \end{bmatrix}. \quad (18)$$

Because we assume that the angular momentum of the overall system is zero, if the angular momentum of the CMG about the  $Y_c$ -axis is zero, then the angular velocity of the satellite about the  $Z_b$ -axis is also zero. In such a case, by ignoring the gyration, the equation of motion can be approximated to describe two-axis rotation about the  $X_b$ - and  $Y_b$ -axes as

$$\begin{bmatrix} J_x & 0 \\ 0 & J_y \end{bmatrix} \begin{bmatrix} \dot{\omega}_1 \\ \dot{\omega}_2 \end{bmatrix} = -h_0 \begin{bmatrix} -c\beta c\delta_1 & c\beta c\delta_3 \\ s\beta c\delta_1 & s\beta c\delta_3 \end{bmatrix} \begin{bmatrix} \dot{\delta}_1 \\ \dot{\delta}_3 \end{bmatrix} \quad (19)$$

which can be rewritten as

$$\tilde{\mathbf{J}}\dot{\boldsymbol{\omega}} = -h_0\tilde{\mathbf{A}} \begin{bmatrix} \dot{\delta}_1 \\ \dot{\delta}_3 \end{bmatrix} \quad (20)$$

where

$$\tilde{\mathbf{A}} = \begin{bmatrix} -c\beta c\delta_1 & c\beta c\delta_3 \\ s\beta c\delta_1 & s\beta c\delta_3 \end{bmatrix}. \quad (21)$$

If we let  $v = |\dot{\omega}|^2$ , then the differential equation Eq. (16) can be rewritten as

$$\dot{v} = (1+v)(\dot{\boldsymbol{\omega}} \cdot \boldsymbol{\omega}). \quad (22)$$

Introducing the virtual angular velocity

$$\hat{\omega}_d = -k_1\hat{\omega} \quad (\text{or } \tilde{\omega}_d = -k_1\boldsymbol{\omega}), (k_1 > 0), \quad (23)$$

and substituting  $\tilde{\omega}_d$  into  $\tilde{\omega}$  in Eq. (22), Eq. (22) then becomes

$$\dot{v} = -k_1(1+v)v (< 0). \quad (24)$$

The solution of the above differential equation is then

$$v = |\dot{\omega}|^2 = |\boldsymbol{\omega}|^2 = 1/(\gamma e^{k_1 t} - 1) \quad (25)$$

where  $\gamma$  is an integration constant. As shown in Eq. (25), the parameter  $v(=|\dot{\omega}|^2)$  is asymptotically stable. The virtual angular velocity (Eq. (23)) is input to stabilize the body axis  $Z_b$  to the inertial  $Z$ -axis. In this paper, we consider the task of pointing  $Z_b$  in the target direction starting from an arbitrary direction in

the inertial coordinate system. For simplicity, we take the  $Z$ -axis of the inertial coordinate system as the target LOS direction without loss of generality.

In order to derive a steering control law that is intended to follow the virtual angular velocity input (Eq. (23)), by introducing the difference between the current angular velocity vector and the virtual angular velocity input as  $\boldsymbol{\sigma} = \tilde{\boldsymbol{\omega}} - \tilde{\boldsymbol{\omega}}_d$ , a Lyapunov function candidate is chosen as

$$V(v, \boldsymbol{\sigma}) = v + \frac{1}{2}\boldsymbol{\sigma}^T\boldsymbol{\sigma} = v + \frac{1}{2}|\tilde{\boldsymbol{\omega}} - \tilde{\boldsymbol{\omega}}_d|^2. \quad (26)$$

The satellite angular acceleration due to the CMG-generated torque is transformed to the satellite's body coordinate system, noting that the angular acceleration about the  $Z_c$ -axis is also close to zero, we have

$$\dot{\boldsymbol{\omega}} = \tilde{\mathbf{R}}\dot{\boldsymbol{\omega}} = -h_0\tilde{\mathbf{J}}^{-1}\tilde{\mathbf{A}} \begin{bmatrix} \dot{\delta}_1 \\ \dot{\delta}_3 \end{bmatrix} \quad (27)$$

where

$$\tilde{\mathbf{R}} = \begin{bmatrix} 1 & 0 & 0 \\ 0 & 1 & 0 \end{bmatrix}. \quad (28)$$

In addition, note that

$$\tilde{\boldsymbol{\omega}} = \tilde{\boldsymbol{\omega}}_d + \boldsymbol{\sigma}, \quad (29)$$

$$\dot{\tilde{\boldsymbol{\omega}}}_d = -k_1\dot{\boldsymbol{\omega}} = -k_1\tilde{\mathbf{W}}\boldsymbol{\omega} \quad (30)$$

where

$$\tilde{\mathbf{W}} = \begin{bmatrix} (1+w_1^2-w_2^2)/2 & w_1w_2 & w_2 \\ w_1w_2 & (1-w_1^2+w_2^2)/2 & -w_1 \end{bmatrix}. \quad (31)$$

By taking the time derivative of Eq. (26) and substituting Eqs. (27), (29), and (30), we have

$$\dot{V} = -k_1(1+v)v + \boldsymbol{\sigma} \cdot \left\{ (1+v)\boldsymbol{\omega} + (k_1\tilde{\mathbf{W}}\boldsymbol{\omega} - h_0\tilde{\mathbf{J}}^{-1}\tilde{\mathbf{A}}\dot{\boldsymbol{\delta}}) \right\}. \quad (32)$$

If a steering control law is designed as

$$\begin{bmatrix} \dot{\delta}_1 \\ \dot{\delta}_3 \end{bmatrix} = \frac{1}{h_0}\tilde{\mathbf{A}}^{-1}\tilde{\mathbf{J}} \left\{ k_1\tilde{\mathbf{W}}\boldsymbol{\omega} + k_2(\tilde{\mathbf{R}}\boldsymbol{\omega} + k_1\boldsymbol{\omega}) + (1+v)\boldsymbol{\omega} \right\} \quad (33)$$

then

$$\dot{V} = -k_1(1+v)v - k_2|\boldsymbol{\sigma}|^2 \leq 0. \quad (34)$$

As we assume the application of feedback control near the target LOS and consider  $\delta_1 \approx \delta_3 \approx 0$  or  $\pi$ , we have  $c\delta_1 \neq 0$  and  $c\delta_3 \neq 0$ . We then have  $|\tilde{\mathbf{A}}| \neq 0$ , and it is always possible to calculate the gimbal steering law (Eq. (33)). In short, the steering control law (Eq. (33)) does not encounter singularities near the target LOS.

Consequently,  $V$  is radially unbounded,  $\dot{V} < 0 \forall (v, \boldsymbol{\sigma}^T)^T \in \mathcal{R}^3 \setminus \{\mathbf{0}\}$ , and  $V(\mathbf{0}) = 0$ . This proves that the steering control law employed near the target LOS can asymptotically stabilize the current LOS to the target LOS. Hereinafter, the above steering control law (Eq. (33)) is referred to as "steering control law-1."

## 4.2. Damping of rotation about the LOS axis

In micro-gravity experiments using parabolic flight, the airplane changes its flight direction from upward to downward before providing micro-gravity conditions. This change in the flight direction then induces the relative pitch-up motion in the cabin for the experiments. Hereinafter, for simplicity, the  $X_b$ -axis is coincident with the  $x$ -axis of the airplane at the initial time of the experiments. If the satellite model does not rotate relative to the airplane body at the initial time of the micro-gravity experiment, the satellite model will have an initial angular velocity about the pitch axis of the airplane. It is desirable, but very difficult, to set the initial angular velocity of the satellite model to zero before experiments under micro-gravity conditions, particularly the angular velocity about the  $Z_b$ -axis of the satellite model due to the pitching motion of the airplane. In order to address this problem, we consider the compensation of the rotational motion about the  $Z_b$ -axis using the 2nd and 4th CMGs in this study.

When the 2nd and 4th gimbals are actuated in the direction opposite the origin, such that  $[\delta_2 \ \delta_4] = [\delta \ -\delta]$ , no torque is generated about the  $X_b$ - and  $Y_b$ -axes, but the torque about the  $Z_b$ -axis is generated as

$$\tau = -2h_0\delta c\beta \cos \delta . \quad (35)$$

In order to damp out the angular velocity about the  $Z_b$ -axis, let us consider the following feedback control torque about the  $Z_b$ -axis:

$$\tau = -k_3 J_z \omega_3 . \quad (36)$$

Now, we assume that the initial gimbal angles of the 2nd and 4th CMGs are both zero. In this case, a steering law for the 2nd and 4th gimbal to damp out the angular velocity about the  $Z_b$ -axis is derived from Eqs. (35) and (36) as follows:

$$\begin{bmatrix} \dot{\delta}_2 \\ \dot{\delta}_4 \end{bmatrix} = \frac{k_3 J_z \omega_3}{2h_0 c\beta} \begin{bmatrix} \frac{1}{\cos \delta_2} \\ \frac{-1}{\cos \delta_2} \end{bmatrix} . \quad (37)$$

In this study, the steering control law combining Eq. (33) and Eq. (37) is referred to as ‘‘steering control law-2.’’

By taking into consideration the mechanical limitation for the gimbal motors and singularity avoidance, the following constraints are set on the gimbal rate in accordance with the gimbal rate and angles.

$$\dot{\delta}_i = \begin{cases} \text{sat}_{\delta_{\max}}(\dot{\delta}_i) & |\delta_i| < \delta_{\max} \\ 0 & \delta_i \geq \delta_{\max}, \dot{\delta}_i > 0 \\ 0 & \delta_i \leq -\delta_{\max}, \dot{\delta}_i < 0 \end{cases} \quad (38)$$

## 5. Numerical Simulation and Experiments

### 5.1. Experimental setup

Figure 4 shows the satellite model used in this study. Table 1 shows the parameters of the satellite model: size, weight, moment of inertia, CMG wheel angular momentum, and constraints on the gimbal rate and angles to avoid singularities. The moment of inertia about each axis, ( $J_x, J_y, J_z$ ), was measured by a torsional pendulum method, which is described as:

$$J = \frac{mgd^2T^2}{4\pi^2L} \quad (39)$$

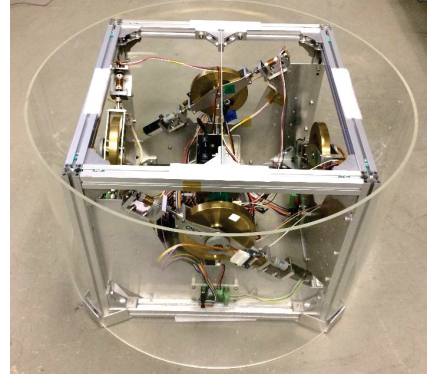


Fig. 4. Experimental setup.

Table 1. System model.

Parameter	Values
Size	radius 0.25 [m], height 0.35 [m]
Mass $m$	10.0 [kg]
$J$	diag(0.238, 0.341, 0.268) [kgm <sup>2</sup> ]
$J_w$	0.00083 [kgm <sup>2</sup> ]
$\Omega$	2000 [rpm] (= 209.44 [rad/s])
$h_0 = J_w\Omega$	0.02 [Nms]
$\dot{\delta}_{\max}$	30.0 [deg/s]
$\delta_{\max}$	65.0 [deg]

Table 2. Simulation and experiments parameters.

Parameter	Values
$w_1(0), w_2(0), z(0)$	(0.1895, 0.1895, 0.0)
Control gains $k_1, k_2, k_3$	3.0, 3.0, 4.0
Initial gimbal angles $\delta(0)$	$[0, 0, 0, 0]^T$ [rad]

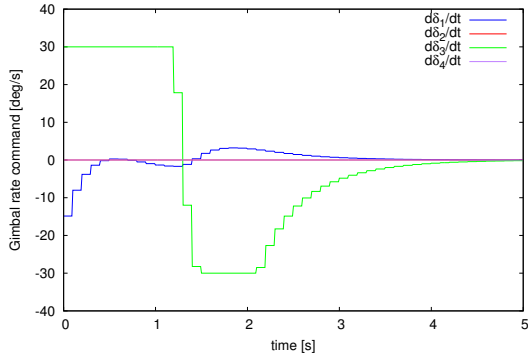
where  $m$  is the mass of the model [kg],  $d$  is the distance between two suspending cables [m],  $T$  is the oscillation period [s], and  $L$  is the length of the cables [m]. The CMG wheels are made of brass, and their radius is 10 cm. The moment of inertia of the CMG wheel was measured using a moment of inertia measurement device (MOI-005-104, Inertia Dynamics and LLC Co.).

The control laws are implemented in a laptop computer (PC) using Matlab<sup>®</sup> code. The angular velocities are measured by mems gyros. The gimbal angles are measured using potentiometers. Arduino Mega is used as an on-board computer to control the stepper motors for gimbal angles and direct-current (DC) motors for the wheels and to communicate with the PC.

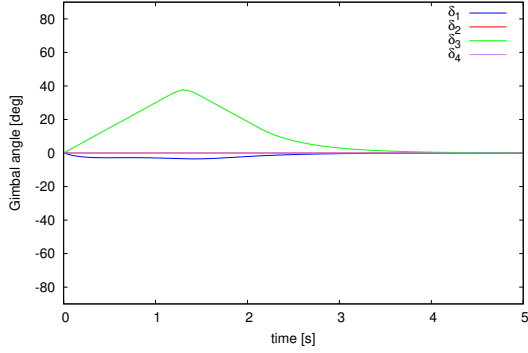
The data of the angular velocities and gimbal angles are sent from the satellite model to the PC, and the gimbal rate command determined by the steering control laws is sent from the PC to the satellite model. This communication is implemented by serial communication via Bluetooth with 38,400 bps. The  $W$ - $Z$  parameters to express the attitude are calculated in the PC by integrating Eq. (11) using the angular velocities measured by the mems gyros. The experimental results are recorded in the form of CSV files in the PC. The sampling period in the experiments is approximately between 0.08 s and 0.1 s.

### 5.2. Numerical and experimental results

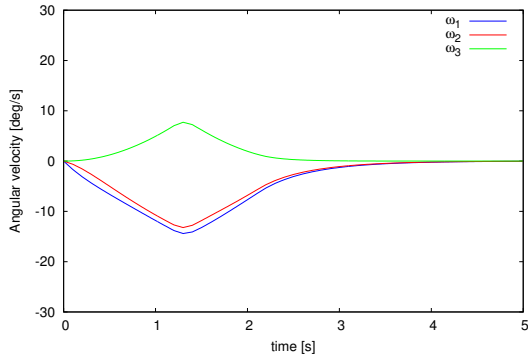
It is desirable to appropriately choose attitude maneuver angles and control gains to perform experiments within the available length of time for free-floating in the micro-gravity condition. The technical staff of Diamond Air Service Inc. suggested that, although the micro-gravity condition continues for



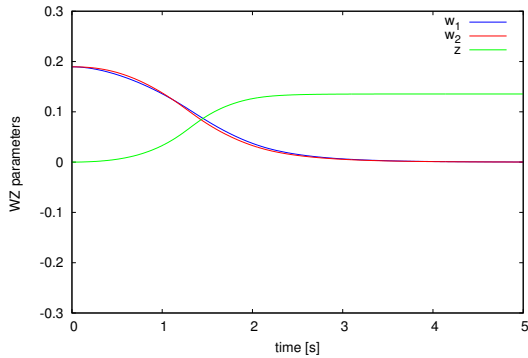
(a) Gimbal rate command



(b) Gimbal angles

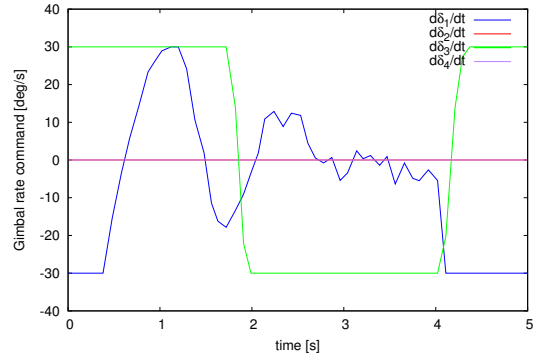


(c) Angular velocities

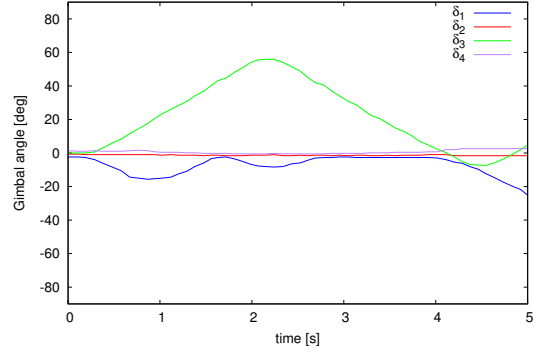


(d) W-Z parameters

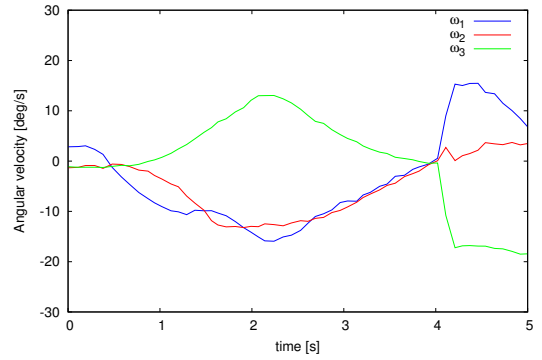
Fig. 5. Simulations results for steering control law-1.



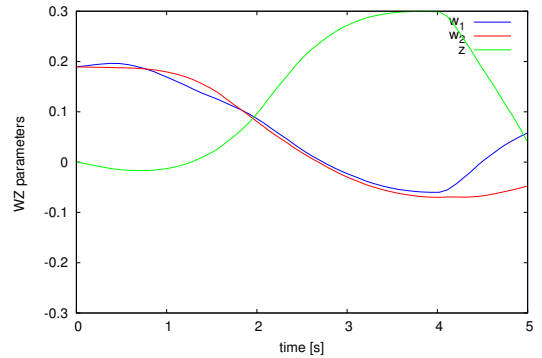
(a) Gimbal rate command



(b) Gimbal angles



(c) Angular velocities



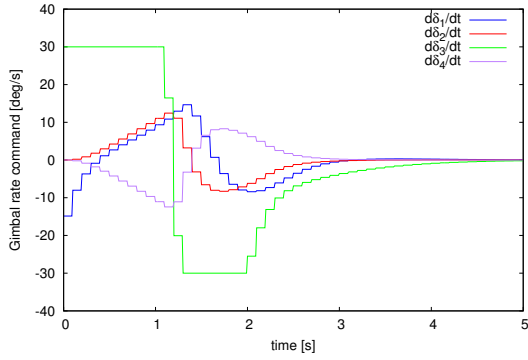
(d) W-Z parameters

Fig. 6. Experimental results for steering control law-1.

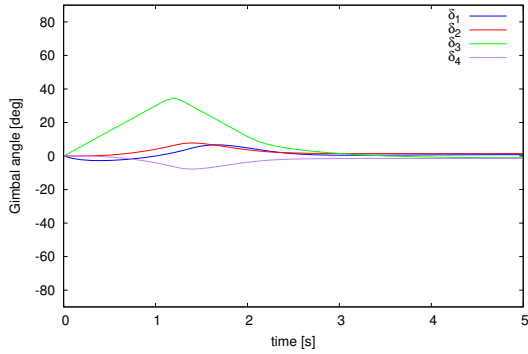
approximately 20 s, the length of time for free-floating experiments will be limited to within 5 s due to the translational motion of the model in the free space of the cabin. By taking this suggestion into consideration, we developed the experimental setup described above, and selected the initial W-Z parameters and control gains. Table 2 shows the selected initial W-Z pa-

rameters and control gains for the experiments. The initial W-Z parameters correspond to an angle of 30 deg between the  $X_b$ - $Y_b$  axes. In other words, we intend to perform an attitude maneuver of 30 deg between the  $X_b$ - $Y_b$ -axes.

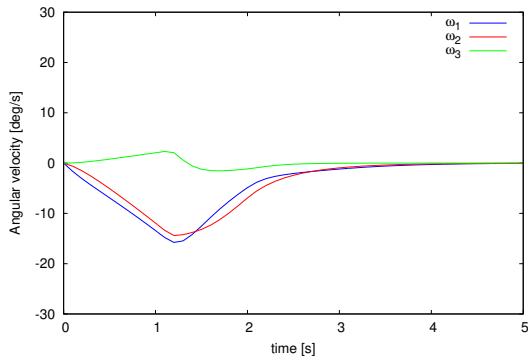
Although the sampling period in the experiments varies between 0.08 s and 0.1 s due to the communication condition and



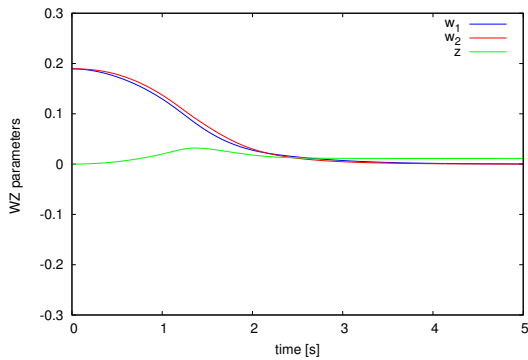
(a) Gimbal rate command



(b) Gimbal angles

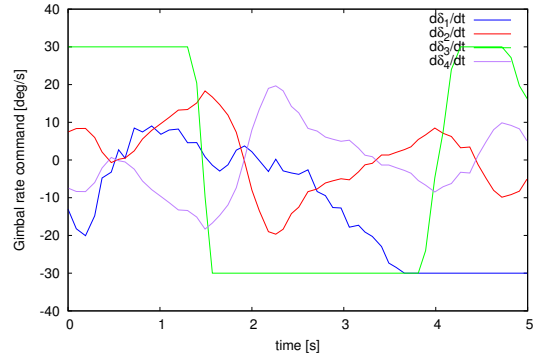


(c) Angular velocities

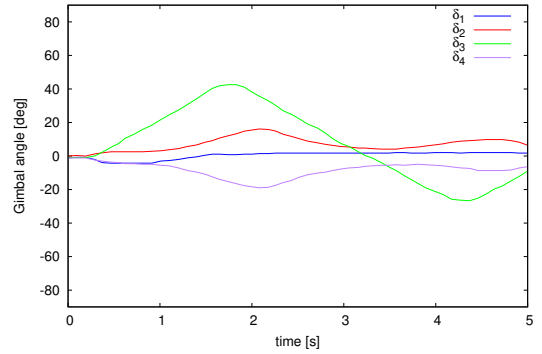


(d) W-Z parameters

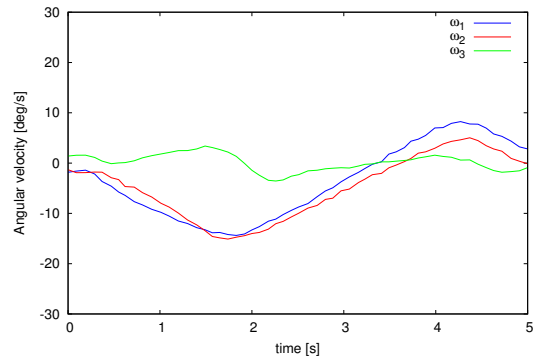
Fig. 7. Simulations results for steering control law-2.



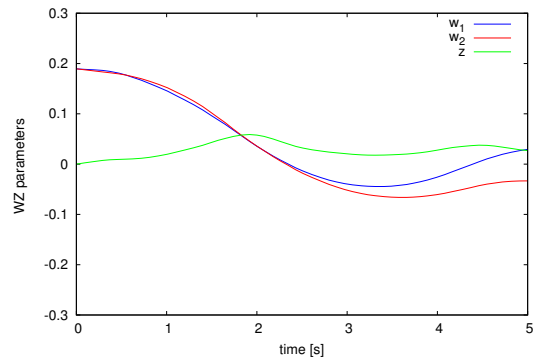
(a) Gimbal rate command



(b) Gimbal angles



(c) Angular velocities



(d) W-Z parameters

Fig. 8. Experimental results for steering control law-2.

the task load on the PC, in the numerical simulations, the sampling period of the gimbal rate command is set to 0.1 s in order to simply emulate the experiments.

Firstly, we present and discuss the numerical results for steering control law-1. Figure 5 shows the result of simulation for steering control law-1. The third gimbal rate is dramatically

switched from the maximum positive rate to a negative rate around 1.3 s and then gradually changed to zero after 2.0 s. In contrast, the first gimbal rate changed smoothly. As shown in Figs. 5(c) and 5(d), the LOS can be pointed to and stabilized to the target LOS direction by two skewed SGCMGs with the feedback steering control law described herein, and the settling

time of the attitude maneuver is approximately 4.0 s, which is expected for the experiment. As mentioned in the previous subsection, steering control law-1 neither damps out the rotational motion about the LOS direction nor stabilizes the attitude angle around the LOS axis to zero. As a result, the attitude around the LOS direction, which corresponds to the  $Z$  parameter, shifted from the initial attitude, as shown in Fig. 5(d). This attitude shift around the LOS axis is approximately 0.13 rad (= 7.4 deg).

Figure 6 shows the results of experiment for steering control law-1. Similar to the numerical result, the third gimbal rate is switched from the maximum positive rate to the negative rate, but swift timing is delayed from the numerical result. In addition, the third gimbal rate does not approach zero. As shown in Fig. 6(a), the first gimbal rate in the experiment exhibits a trend of changing from a negative value to positive value. This trend is similar to that of the numerical experiment, but the rate magnitude is greater than the numerical result. The angular velocities approached zero around 4 s, as shown in Fig. 6(c), but suddenly changed. This sudden change resulted from the collision of the model with the wall of the cabin. Thus, this sudden change can be ignored. The LOS is stabilized approximately to zero around 4 s, as shown in Fig. 6(d). This setting is similar to the time for the numerical results. As shown in Fig. 6(d), the attitude shift around the LOS axis is approximately 0.3 rad (= 17.2 deg), which is approximately 2.5 times the numerical result. Although there are some differences between the numerical and experimental results, it is experimentally confirmed that steering control law-1 can stabilize the LOS to the target LOS direction.

Next, we present and discuss the results for steering control law-2. As mentioned above, the attitude around the LOS axis ( $Z$  parameter) shifted from the initial attitude for the case of steering control law-1, because steering control law-1 neither damps out rotational motion about the LOS direction nor stabilizes the attitude angle around the LOS direction to zero. In contrast, steering control law-2 was designed to suppress rotation around the LOS direction. In order to validate this effect of steering control law-2, numerical simulations and experiments are carried out. Figures 7 and 8 show the results of the numerical simulations and the experiments using steering control law-2, respectively. In contrast to the results for steering control law-1, all of the gimbals are actuated. The 2nd and 4th gimbals are actuated in opposite directions in order to suppress the rotational motion around the LOS axis, as shown in Figs. 7(a) and 8(a), but the magnitude of the 2nd and 4th gimbal rate is larger than that of the numerical simulation. The trend of the gimbal rate change in the experiment is similar to that of the numerical result until approximately 2.2 s, but the first and third gimbal rates in the experiment differed from those of the numerical simulation. In addition, in the experiment, the first gimbal rate command was negative after approximately 2.5 s, but the first gimbal angle was not correctly actuated. This may be because of communication or mechanical trouble during the experiment. Despite this trouble in the first gimbal motion, Fig. 8(d) shows that the LOS maneuvering to the target LOS direction was completed in approximately 4 s in the experiment. This is because the angular momentum of the third CMG can be in the direction between the  $X_b$ - and  $Y_b$ -axes by tilting the gimbal, and this leads to easy maneuvering around the direction between the  $X_b$ - and

$Y_b$ -axes. In other words, the third CMG played the most important role in maneuvering between the  $X_b$ - and  $Y_b$ -axes. In addition, steering control law-2 succeeded in damping out the angular velocity about the LOS axis, as shown in Figs. 7(c) and 8(c). This effect of steering control law-2 resulted in the suppression of the attitude drift about the LOS axis, as shown in Figs. 7(d) and 8(d).

## 6. Conclusion

In this paper, the  $W$ - $Z$  parameters are used to express the attitude, and two steering feedback-control laws are derived for LOS maneuver control, based on a backstepping control method. The first control law was designed for LOS angle stabilization only, and the second control law was designed not only for LOS angle stabilization but also for suppression of rotation around the LOS axis.

Taking into consideration the available length of time for experiments under micro-gravity conditions, an experimental setup that possesses a large angular momentum was developed and control gains and the maneuver angle were selected.

In order to validate the steering control laws, numerical simulations and experiments under micro-gravity conditions were carried out, and the obtained results were compared. As a result, the second steering control law, which was designed to suppress the attitude drift about the LOS axis, can suppress the attitude rotation shift about the LOS axis, and although there were some differences between the numerical and experimental results, due primarily to trouble in the first gimbal motion, the steering control laws presented in this study can stabilize the initial LOS direction to the target LOS direction.

## Acknowledgments

This study was supported by a Grant-in-Aid for Scientific Research (B) (No. 25289309) from JSPS. The authors would like to express their gratitude to Diamond Air Service Inc. for providing the micro-gravity environment for this study.

## References

- 1) Crouch, P. E.: Spacecraft Attitude Control and Stabilization: Application of Geometric Control Theory to Rigid Body Model, *IEEE Trans. Automatic Control*, **29**(1984), pp.321–331.
- 2) Aeyels, D.: Stabilization by Smooth Feedback Control of the Angular Velocity of a Rigid Body, *Systems & Control Letters*, **6**(1985), pp.59–63.
- 3) Aeyels, D. and Szafranski, M.: Comments on the Stabilizability of the Angular Velocity of a Rigid Body, *Systems & Control Letters*, **10**(1988), pp.35–39.
- 4) Sontag, E.D. and Sussman, H.J.: Further Comments on the Stabilizability of the Angular Velocity of a Rigid Body, *Systems & Control Letters*, **12**(1988), pp.213–217.
- 5) Astolfi, A. and Rapaport, A.: Robust Stabilization of the Angular Velocity of a Rigid Body, *Systems & Control Letters*, **34**(1998), pp.257–264.
- 6) Astolfi, A.: Output Feedback Stabilization of the Angular Velocity of a Rigid Body, *Systems & Control Letters*, **36**(1999), pp.181–192.
- 7) Mazenc, F. and Astolfi, A.: Robust Output Feedback Stabilization of the Angular Velocity of a Rigid Body, *Systems & Control Letters*, **39**(2000), pp.203–210.
- 8) Outbib, R. and Sallet, G.: Stabilizability of the Angular Velocity of a

- Rigid Body Revisited, *Systems & Control Letters*, **18**(1992), pp.93–98.
- 9) Andriano, A.: Global Feedback Stabilization of the Angular Velocity of a Symmetric Rigid Body, *Systems & Control Letters*, **20**(1993), pp.361–364.
  - 10) Kojima, H.: Stabilization of Angular Velocity of Asymmetrical Rigid Body using Two Constant Torques, *Journal of Guidance, Control, and Dynamics*, **30**(2007), pp.1163–1168.
  - 11) Byrnes, C. I. and Isidori, A.: On the Attitude Stabilization of Rigid Spacecraft, *Automatica*, **27**(1991), pp.87–95.
  - 12) Coron, J. M. and Kerai, E.Y.: Explicit Feedbacks Stabilizing the Attitude of a Rigid Spacecraft with Two Control Torques, *Automatica*, **32**(1996), pp.669–677.
  - 13) Krishnan, H., Reyhanoglu, M. and McClamroch, H.: Attitude Stabilization of a Rigid Spacecraft Using Two Control Torques: A Nonlinear Control Approach Based on the Spacecraft Attitude Dynamics, *Automatica*, **30**(1994), pp.1023–1027.
  - 14) Morin, P., Samson, C., Pomet, J. B. and Jiang, Z. P.: Time-Varying Feedback Stabilization of the Attitude of a Rigid Spacecraft with Two Controls, *Systems & Control Letters*, **25**(1995), pp.375–385.
  - 15) Morin, P. and Samson, C.: Time-Varying Exponential Stabilization of a Rigid Spacecraft with Two Control Torques, *IEEE Transactions on Automatic Control*, **42**(1997), pp.528–533.
  - 16) Tsiotras, P., Corless, M. and Longuski, M.: A Novel Approach to the Attitude Control of Axisymmetric Spacecraft, *Automatica*, **31**(1995), pp.1099–1112.
  - 17) Tsioras, P. and Longuski, J. M.: Spin-Axis Stabilization of Symmetric Spacecraft with Two Control Torques, *Systems & Control Letters*, **23**(1994), pp.395–402.
  - 18) Tsiotras, P.: Optimal Regulation and Passivity Results for Axisymmetric Rigid Bodies Using Two Controls, *Journal of Guidance, Control, and Dynamics*, **20**(1997), pp.457–464.
  - 19) Tsiotras, P. and Luo, J.: Reduced Effort Control Laws for Underactuated Rigid Spacecraft, *Journal of Guidance, Control, and Dynamics*, **20**(1997), pp.1089–1095.
  - 20) Kwon, S., Shimomura, T. and Okubo, H.: Pointing Control of Spacecraft Using Two SGCMGs via LPV Control Theory, *Acta Astronautica*, **68**(2011), pp.1168–1175.
  - 21) Gui, H., Jin, L. and Xu, S.: Local Controllability and Stabilization of Spacecraft Attitude by Two Single-gimbal Control Moment Gyros, *Chinese J Aeronautics*, **26**(2013), pp.1218–1226.
  - 22) Gui, H., Vukovich, G., and Xu, S.: Attitude Stabilization of a Spacecraft with Two Parallel Control Moment Gyroscopes, *Journal of Guidance, Control, and Dynamics*, **39**(2016), pp.724–732.
  - 23) Yamada, K., Jikuya, I., and Kwak, O.: Rate Damping of a Spacecraft Using Two Single-Gimbal Control Moment Gyros, *Journal of Guidance, Control, and Dynamics*, **36**(2013), pp.1606–1623.
  - 24) Kasai, S., Kojima, H., and Satoh, M.: Spacecraft Attitude Maneuver using Two Single-gimbal Control Moment Gyros, *Acta Astronautica*, **84**(2013), pp.88–98.
  - 25) Gui, H., Jin, L., Xu, S. and Hu, Q.: Attitude Stabilization of a Spacecraft by Two Skew Single-Gimbal Control Moment Gyros, AIAA 2013-4794, 2013.
  - 26) Kojima, H., Trivailo, P., and Yoshimura, Y.: Spacecraft Line of Sight Maneuver Control Using Skew-arrayed Two Single-Gimbal Control Moment Gyros, *Transactions of JSASS, Aerospace Technology Japan*, **14**, ists30 (2016), pp.Pd.31–Pd.37.
  - 27) Tsiotras, P. and Longuski, J. M.: A New Parameterization of the Attitude Kinematics, *J. Astronautical Science*, **41**(1995), pp.243–262.
  - 28) Schwartz, J. L.: Historical Review of Air-Bearing Spacecraft Simulators, *Journal of Guidance, Control, and Dynamics*, **26**(2003), pp.513–522.
  - 29) <http://www.das.co.jp/service/operation/gravity/index.html> (accessed March 20, 2017).